Ultrahigh spontaneous emission extraction efficiency induced by evanescent wave coupling

X.-L. Wang,[1,a)] S. Furue,[1] M. Ogura,[1] V. Voliotis,[2,b)] M. Ravaro,[2] A. Enderlin,[2] and R. Grousson[2]
[1]*Nanotechnology Research Institute, National Institute of Advanced Industrial Science and Technology (AIST), Tsukuba Central 2, Tsukuba 305-8568, Japan*
[2]*Institut des Nanosciences de Paris, CNRS UMR 7588, Université Pierre et Marie Curie, Campus Boucicaut, 140 rue de Lourmel, 75015 Paris, France*

(Received 7 January 2009; accepted 2 February 2009; published online 3 March 2009)

A spontaneous emission extraction efficiency greater than 50% is observed in a GaAs/AlGaAs quantum well structure grown on the subwavelength-sized ridge top facet of a V-grooved substrate by means of photoluminescence study. This is an extraction efficiency about 20 times higher than that of a similar structure grown on a flat substrate. It is demonstrated both experimentally and theoretically that the high extraction efficiency is the result of the efficient conversion of evanescent waves into propagating waves in air through constructive coupling of evanescent waves generated on the two sidewall facets of the V-grooved substrate by total internal reflection. © *2009 American Institute of Physics*. [DOI: 10.1063/1.3086887]

Control of the spontaneous emission of semiconductor materials is of great interest both from the standpoint of basic physics and of improving optoelectronic device performances. For example, efficient extraction of spontaneous emission generated in semiconductors has been proven to be a very challenging task since spontaneous emission tends to be trapped inside semiconductors owing to total internal reflection (TIR) that occurs at the semiconductor-air interface.[1,2] For a planar structure, only light in the narrow escape cone defined by the critical angle for TIR, which accounts for only a few percent of the total emission, can escape to air.[1,2] An important effect accompanying TIR is the formation of an evanescent wave, which propagates only parallel to the semiconductor surface. In the direction normal to the surface, the evanescent wave decays exponentially and is localized in air over a distance of the order of the emission wavelength.[3,4] Up until now, the only known way of transforming an evanescent wave into a propagating wave in air is to scatter the evanescent wave with a subwavelength-sized object placed in contact with the evanescent field.[4–7] Here, we report that the evanescent wave can be transformed into a wave propagating in air with a very high efficiency through a constructive coupling effect of two evanescent waves, which is achieved in a GaAs/AlGaAs quantum well (QWL) structure grown on the subwavelength-sized ridge top facet of a V-shaped substrate. An extraction efficiency of spontaneous emission exceeding 50% was obtained owing to this unique evanescent wave coupling effect.

As illustrated in Fig. 1(a), the sample used in this study is a single $Al_{0.3}Ga_{0.7}As/GaAs/Al_{0.3}Ga_{0.7}As$ QWL structure, sandwiched between two higher Al-content $Al_{0.65}Ga_{0.35}As$ layers (hereafter referred to as "$Al_{0.65}Ga_{0.35}As$ confinement layers"), grown on a 4-μm-pitched, $[1\bar{1}0]$-oriented, V-grooved GaAs substrate by metal organic vapor phase epitaxy.[8] In this structure, the GaAs well layer consists of three different quantum structures depending on crystal facets, that is, a thicker QWL grown on the (001) flat facet, a thinner QWL grown on the (111)*A* sidewall facet, and a crescent-shaped quantum wire (QWR) formed at the V-groove bottom.[8,9] The thicknesses of the (001) flat and (111)*A* sidewall QWLs, as determined through high-resolution transmission electron microscopy (TEM), were about 4.3 and 1.7 nm, respectively. The lateral width and growth thickness of the (001) flat $Al_{0.3}Ga_{0.7}As/GaAs/Al_{0.3}Ga_{0.7}As$ QWL are about 0.5 and 0.6 μm, respectively, and the thickness of the $Al_{0.65}Ga_{0.35}As$ confinement layers is about 0.75 μm at the ridge top [Fig. 1(b)].

Figure 2(a) compares the 4.5 K photoluminescence (PL) spectrum of the sample described above with that of a similar structure grown on a flat substrate. In the PL measurement of the V-grooved sample, the wavelength of a Ti:sapphire excitation laser (normal incidence, spot size of

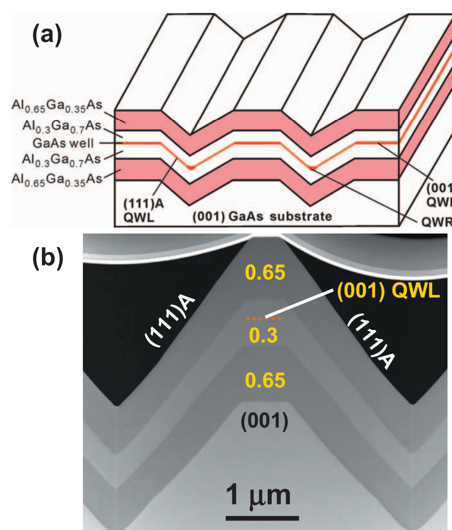

FIG. 1. (Color) Schematic drawing (a) and cross-sectional TEM image (b) of the GaAs/AlGaAs QWL structure used in this study. The red dashed line in the TEM image indicates the position of the (001) QWL.

a)Electronic mail: xl.wang@aist.go.jp.
b)Also at Université Evry Val d'Essonne, Boulevard F. Mitterand, 91025 Evry, France.

© 2009 American Institute of Physics
Downloaded 17 Mar 2009 to 129.8.242.67. Redistribution subject to AIP license or copyright; see http://apl.aip.org/apl/copyright.jsp

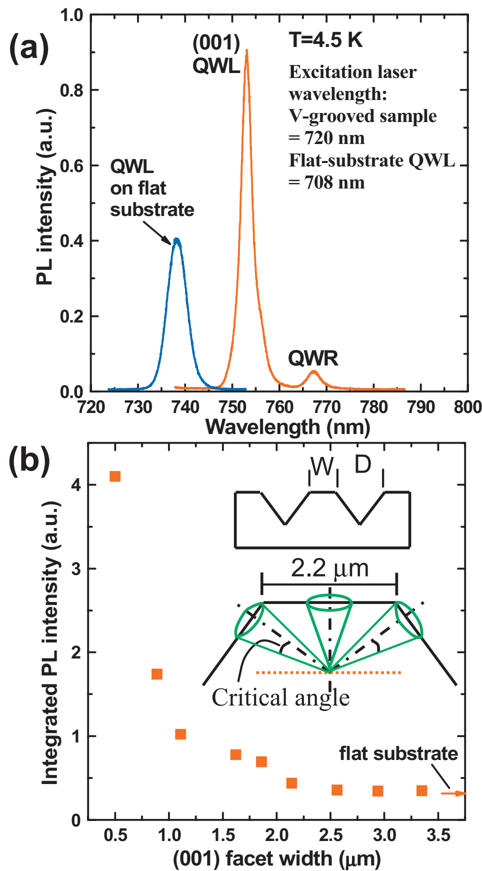

FIG. 2. (Color) (a) Comparison of PL spectrum of the sample shown in Fig. 1(b) with that of a similar sample grown on a flat substrate measured at 4.5 K. (b) Integrated PL intensities of the (001) QWL as a function of the (001) facet width *W*. The lower inset shows the development of the escape cones for the sample with 2.2-μm-wide (001) facet, where the dashed lines indicate the surface normal.

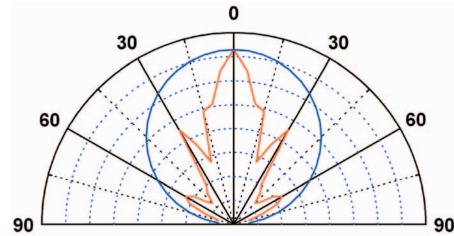

FIG. 3. (Color) Polar plot of angle-resolved PL intensity of the sample shown in Fig. 1(b) measured in the direction perpendicular to the V-groove stripe. The blue curve gives the calculated Lambertian emission pattern of a flat-substrate sample.

≈ 65 μm, and power density of ≈ 226 W/cm^2) was tuned to be longer than the (111)*A* QWL emission wavelength (~ 704 nm), and thus only the (001) QWL and the V-groove bottom QWR were excited selectively. The strong and the weak peaks were attributed to luminescence from the (001) QWL and the QWR, respectively.[8,10] It is very surprising that the (001) QWL, with a surface occupation ratio of only about 12.5% (=0.5/4), showed an integrated PL intensity about 1.6 times stronger than that of the flat substrate sample. We would like to point out that the actual intensity ratio should be even larger since part of the incident beam is diffracted by the intersection between the (001) and the (111)*A* facets, which will reduce the laser excitation efficiency of the V-grooved sample. It was also found that the PL intensity is very sensitive to the lateral width of the (001) facet. Figure 2(b) shows the integrated PL intensity of the (001) QWL as a function of the (001) facet width *W*, where the PL intensities were normalized to unit (001) QWL area. For this experiment, a series of V-grooved substrates with different (001) facet width *W* and constant V-groove opening *D* were fabricated (the upper inset). As can be seen in Fig. 2(b), the integrated PL intensity drops rapidly when the (001) facet width is increased from 0.5 to about 1 μm. Beyond 1 μm, the PL intensity decrease becomes much slower and eventually saturates at a value about 11.7 times lower than that for the 0.5-μm-wide sample. Temperature-dependent PL measurements have confirmed the internal quantum efficiencies of all these samples to be 100% at 4.5 K.[11] Thus, the above difference in PL intensity essentially reflects the difference in light extraction efficiency.

We next estimated the light extraction efficiency of the sample in Fig. 1(b) by using the PL intensity ratio of this sample to the 2.2-μm-wide sample. As will be discussed later, finite-difference time-domain (FDTD) simulation has confirmed that the light extraction process of the 2.2-μm-wide sample is governed by the conventional TIR mechanism. Simple geometrical examination shows that at least two escape cones are developed [the lower inset of Fig. 2(b)] in this sample: one full escape cone on the (001) flat facet and two larger-than-half cones on the two sidewall facets. The amount of light that can be extracted from one escape cone is given by $(1\text{-}\cos\,\theta_c)/2$,[1,2] where θ_c is the critical angle for TIR and equals $\sin^{-1}\,1/n$ with n being the refractive index of the material. Using a refractive index of $n=3.15$ for $Al_{0.65}Ga_{0.35}As$ (at 4.5 K and 750 nm),[12,13] the extraction efficiency of a single escape cone was calculated to be about 2.6%. Thus, the total light extraction efficiency of the 2.2-μm-wide sample should be at least $2\times 2.6\% = 5.2\%$. Using this value and an integrated PL intensity ratio of 9.6 for these two samples, we finally obtained a light extraction efficiency for the 0.5-μm-wide sample in excess of 5.2% $\times 9.6 \approx 50\%$. This is a light extraction efficiency approximately 20 times higher than that of a similar structure grown on a flat substrate.

It is well known that the spontaneous emission can be controlled by modifying the local densities of electromagnetic modes around an emitter, as demonstrated in microcavities and photonic crystals.[14–16] The great enhancement of spontaneous emission extraction efficiency observed in samples with submicron-wide (001) facets suggests the existence of strong nonuniformity in the spatial distribution of electromagnetic mode densities around the ridge top facet. To gain insight into the spatial distribution of electromagnetic mode density of samples showing high light extraction efficiency, we investigated the spatial distribution of PL intensities of the 0.5-μm-wide sample by means of angle-resolved PL measurements. Figure 3 shows the polar plot of the angle-resolved PL intensity measured in the direction perpendicular to the V-groove stripe at 8 K. One can see that the emission pattern is composed of several very sharp emission lobes: one strong lobe in the direction normal to the (001) facet and two weak lobes on either side, about 30° and 60° away from the strong lobe. This emission pattern is completely different from the Lambertian pattern of a flat substrate sample (indicated by the blue curve in Fig. 3),[1] and

Downloaded 17 Mar 2009 to 129.8.242.67. Redistribution subject to AIP license or copyright; see http://apl.aip.org/apl/copyright.jsp

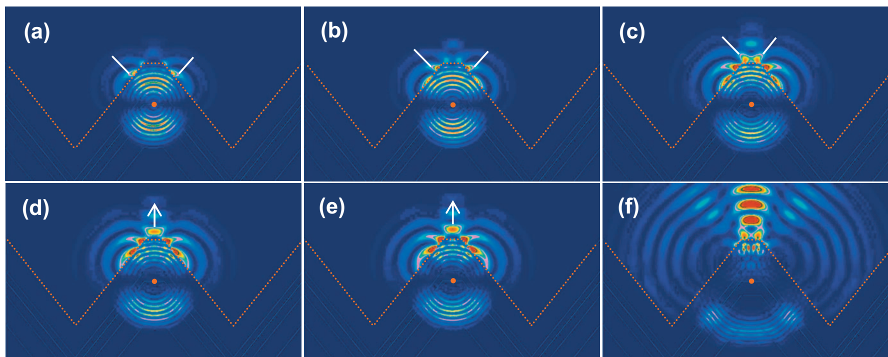

FIG. 4. (Color) Spatial distribution of electromagnetic field intensity around the ridge top facet of the sample shown in Fig. 1(b) calculated by the FDTD method as a function of time: (a) $t=18.67$ fs, (b) $t=19.21$ fs, (c) $t=20.37$ fs, (d) $t=20.54$ fs, (e) $t=20.71$ fs, and (f) $t=25.55$ fs. The red dashed lines represent the position of the sample-air interface.

clearly indicates the existence of spatial nonuniformity in mode densities of electromagnetic waves.

Next, in order to obtain further confirmation of the existence of the localized spatial distribution of electromagnetic modes and to understand the formation mechanism involved, a theoretical calculation of the electromagnetic field around the ridge top facet was performed using the FDTD method. In the simulation, a point source from an electric dipole oriented in the in-plane direction,[17] in the form of a short pulse, was placed in the center of the (001) QWL. Shown in Fig. 4 is a series of calculated images demonstrating the evolution of electromagnetic field with time. When the uniform wave from the point source (red dots) arrives at the ridge-air interface, two electromagnetic modes spatially localized at the interface, indicated by the white bars in Fig. 4(a), appear on the two (111)*A* facets. These two localized modes were attributed to the evanescent waves induced by TIR since they exhibited all the characteristic features of an evanescent wave: (i) they moved only along the (111)*A* facet surface toward the center of the ridge top and did not propagate in air [Figs. 4(a) and 4(b)]; (ii) they were strongly localized in a region much narrower than the emission wavelength in the direction normal to the (111)*A* facets and; (iii) they always started to appear at a position on the (111)*A* facets that forms an angle of incidence with the (111)*A* facets with respect to the point source comparable to the critical angle for TIR ($\sim 18.5°$). The two evanescent waves couple together when they meet at the ridge top and are transformed into light propagating in air in the direction normal to the (001) facet [Figs. 4(c)–4(e)]. We note that the diffraction effect at the intersection between the (001) and the (111)*A* facets presumably plays an important role in the above coupling process by changing the wave vectors of the two evanescent waves to promote their coupling. At 25.55 fs [Fig. 4(e)], when most of the light has escaped the sample, we can clearly observe three spatially localized emission lobes: one strong lobe in the normal direction of the (001) facet and two weak lateral lobes about 40° from the strong lobe, which is in good agreement with the angle-resolved PL data. These results clearly demonstrate a great enhancement in the density of electromagnetic modes around the ridge top in the direction normal to the (001) facet due to the coupling of evanescent waves. The experimentally observed high spontaneous emission extraction efficiency can thus be explained by the efficient coupling of electronic excitations of the (001) QWL into these spatially localized electromagnetic modes. When the ridge top width is increased beyond the emission wavelength, the two localized modes can no longer couple with each other and we revert to the uniform distribution regime of a flat sample.

In conclusion, we have demonstrated the ultrahigh spontaneous emission extraction efficiencies from GaAs/AlGaAs QWLs grown on the subwavelength-sized ridge top facet of a V-grooved substrate due to a constructive coupling effect of evanescent waves generated on different facets by TIR. We believe that our results have the potential to not only greatly impact the field of nanophotonics, but also to lead to significant improvements in the performance of various optoelectronic devices, in particular, light extraction efficiencies of light-emitting diodes.[1,2]

The authors would like to thank Dr. T. Tokizaki for helpful discussions. Part of this work was financially supported by a Grant-in-Aid No. 17360170 for Scientific Research from the Japan Society for the Promotion of Science.

[1]E. F. Schubert, *Light-Emitting Diodes* (Cambridge University Press, Cambridge, 2007), Chap. 5.
[2]H. Benisty, H. D. Neve, and C. Weisbuch, IEEE J. Quantum Electron. **34**, 1612 (1998).
[3]M. Born and E. Wolf, *Principles of Optics* (Cambridge University Press, Cambridge, 1999), Chap. 1.
[4]F. Fornel, *Evanescent Waves From Newtonian Optics to Atomic Optics* (Springer, Berlin, 2001).
[5]D. W. Pohl, W. Denk, and M. Lanz, Appl. Phys. Lett. **44**, 651 (1984).
[6]E. Betzig and R. J. Chichester, Science **262**, 1422 (1993).
[7]M. Ohtsu, J. Lightwave Technol. **13**, 1200 (1995).
[8]X.-L. Wang and V. Voliotis, J. Appl. Phys. **99**, 121301 (2006).
[9]E. Kapon, D. M. Hwang, and R. Bhat, Phys. Rev. Lett. **63**, 430 (1989).
[10]X.-L. Wang, M. Ogura, and H. Matsuhata, Appl. Phys. Lett. **67**, 3629 (1995).
[11]X.-Q. Liu, X.-L. Wang, and M. Ogura, Appl. Phys. Lett. **79**, 1622 (2001).
[12]D. E. Aspnes, S. M. Kelso, R. A. Logan, and R. Bhat, J. Appl. Phys. **60**, 754 (1986).
[13]S. R. Kisting, P. W. Bohn, E. Andideh, I. Adesida, B. T. Cunningham, G. E. Stillman, and T. D. Harris, Appl. Phys. Lett. **57**, 1328 (1990).
[14]R. K. Chang and A. J. Campillo, *Optical Processes in Microcavities* (World Scientific, Singapore, 1996).
[15]D. Kleppner, Phys. Rev. Lett. **47**, 233 (1981).
[16]E. Yablonovitch, Phys. Rev. Lett. **58**, 2059 (1987).
[17]Similar results were also obtained for a point from an electric dipole oriented along the V-groove axis direction, but in that case the intensities of the side emission lobes are slightly stronger than the case of in-plane orientation.

Downloaded 17 Mar 2009 to 129.8.242.67. Redistribution subject to AIP license or copyright; see http://apl.aip.org/apl/copyright.jsp